

## Traveling time and traveling length in critical percolation clusters

Youngki Lee,<sup>1</sup> José S. Andrade, Jr.,<sup>2</sup> Sergey V. Buldyrev,<sup>1</sup> Nikolay V. Dokholyan,<sup>1</sup> Shlomo Havlin,<sup>3</sup> Peter R. King,<sup>4</sup> Gerald Paul,<sup>1</sup> and H. Eugene Stanley<sup>1</sup>

<sup>1</sup>Center for Polymer Studies and Department of Physics, Boston University, Boston, Massachusetts 02215

<sup>2</sup>Departamento de Física, Universidade Federal do Ceará, 60451-970 Fortaleza, Ceará, Brazil

<sup>3</sup>Minerva Center and Department of Physics, Bar-Ilan University, Ramat Gan, Israel

<sup>4</sup>BP Amoco Exploration, Sunbury-on-Thames, Middlesex, TW16 7LN, United Kingdom  
and Department of Engineering, Cambridge University, Cambridge, United Kingdom

(Received 3 March 1999)

We study traveling time and traveling length for tracer dispersion in two-dimensional bond percolation, modeling flow by tracer particles driven by a pressure difference between two points separated by Euclidean distance  $r$ . We find that the minimal traveling time  $t_{min}$  scales as  $t_{min} \sim r^{1.33}$ , which is different from the scaling of the most probable traveling time,  $\tilde{t} \sim r^{1.64}$ . We also calculate the length of the path corresponding to the minimal traveling time and find  $\ell_{min} \sim r^{1.13}$  and that the most probable traveling length scales as  $\tilde{\ell} \sim r^{1.21}$ . We present the relevant distribution functions and scaling relations. [S1063-651X(99)02809-3]

PACS number(s): 47.55.Mh, 05.60.Cd, 64.60.Ak

The study of flow in porous media has many applications, such as hydrocarbon recovery and ground-water pollution [1–5]. Here we study an incompressible flow on two-dimensional bond percolation clusters [6] at criticality where fluid is injected at point  $A$  and recovered at point  $B$  separated from point  $A$  by Euclidean distance  $r$ . At time  $t=0$  we add a passive tracer [7] at the injection point [8]. We investigate the scaling properties of the distributions of *traveling time*, *traveling length*, *minimal traveling time*, and the length of the path corresponding to the minimal traveling time of the tracer particles. We find new dynamical scaling exponents associated with these distributions.

Our first step is to calculate the pressure difference across each bond by solving Kirchhoff's law, which is equivalent to solving the Laplace equation. The velocity across a given bond is proportional to the pressure difference across the bond; we normalize the velocities assuming the total flow between  $A$  and  $B$  is fixed, independent of the distance between  $A$  and  $B$  and the realization of the porous media [9].

We simulate the flow of tracers using a particle-launching algorithm (PLA) [10], where a tracer particle starting from the injection point  $A$  travels through the medium along a path connected to the recovery point  $B$  [11]. The probability  $p_{ij}$  that a tracer particle at node  $i$  selects an outgoing bond  $(ij)$  is proportional to the velocity of flow on that bond;  $p_{ij} = v_{ij}/\sum_k v_{ik}$ , where the  $k$  summation should be taken over all outgoing bonds, i.e., for  $v_{ik} > 0$ . In this process, the time taken to pass through the bond  $(ij)$  is inversely proportional to the velocity of that bond, i.e.,  $t_{ij} = 1/v_{ij}$ .

We measure the distributions,  $P(\tilde{t})$  and  $P(\tilde{\ell})$ , of the traveling time  $\tilde{t}$  and the traveling length  $\tilde{\ell}$  between  $A$  and  $B$  for 10 000 tracer particles for each realization. We sample over 10 000 different realizations with the two points  $A$  and  $B$  fixed. For each realization, we also find the minimal traveling time and the path, which corresponds to the minimal

traveling time to obtain  $P(t_{min})$  and  $P(\ell_{min})$ . We run the simulation for system size  $L \times L$  where  $L = 1000 \gg r$ , and find a well-defined region where the distributions follow the scaling form [12]

$$P(x) = A_x \left( \frac{x}{x^*} \right)^{-g_x} f \left( \frac{x}{x^*} \right), \quad (1)$$

where  $x$  denotes  $\ell_{min}$ ,  $t_{min}$ ,  $\tilde{\ell}$ , or  $\tilde{t}$ . The normalization constant is given by  $A_x \sim (x^*)^{-1}$  and we find the scaling functions to be of the form  $f(y) = \exp(-a_x y^{-\phi_x})$ . The maximum of the probability is at  $x^*$ . Simulation shows that  $x^*$  has a power-law dependence on the distance  $r$ ,

$$x^* \sim r^{d_x}. \quad (2)$$

The exponents  $\phi_x$  and  $d_x$  are related by  $\phi_x = 1/(d_x - 1)$  [13]. The scaling function  $f$  decreases sharply when  $x$  is smaller than  $x^*$ . The lower cutoff is due to the fact that the traveling distance cannot be smaller than the distance  $r$ .

The path, which takes minimal time, is not always the shortest path. However, we find that the distribution of  $\ell_{min}$  coincides with the distribution of the chemical lengths between points separated by distance  $r$  studied in detail in Ref. [14].

In Figs. 1(a), 2(a), and 3(a), we show the log-log plots of distributions  $P(t_{min})$ ,  $P(\tilde{\ell})$ , and  $P(\tilde{t})$ , respectively. For different distances  $r = 4, 8, 16, 32, 64$ , and 128, we determine the characteristic size  $x^*$  as the peak of the distribution. In Figs. 1(b), 2(b), and 3(b), we plot  $x^*$  versus distance  $r$  in a double logarithmic scale and linear fitting yields the expo-

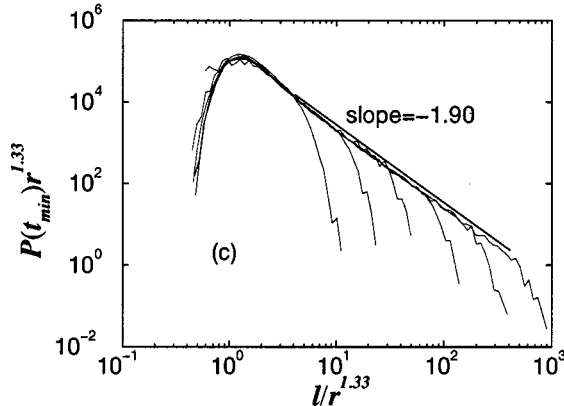
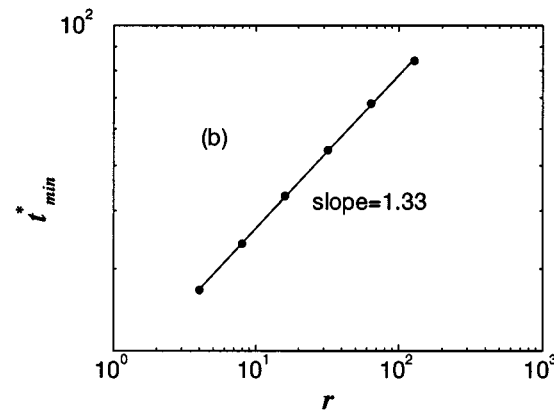
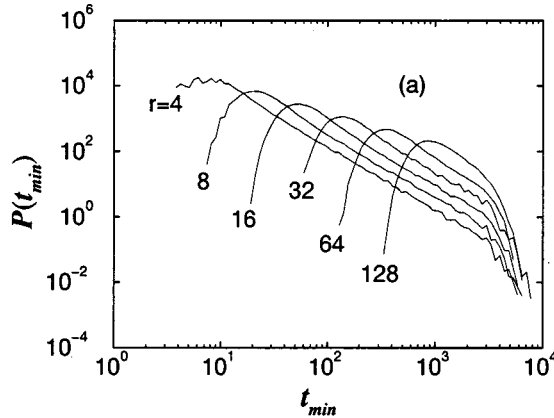


FIG. 1. (a) Log-log plot of the minimal traveling time distribution  $P(t_{min})$  for separations  $r=4, 8, 16, 32, 64$ , and  $128$  between injection and recovery points. (b) Log-log plot of the most probable minimal traveling time versus  $r$ . A linear fit yields  $d_{t_{min}}=1.33\pm 0.05$ . (c) The data obtained by rescaling the minimal time with its characteristic time  $t_{min}^* \sim r^{1.33}$ . A fit of the power-law regime gives  $g_{t_{min}}=1.90\pm 0.05$ .

nents  $d_x$  for each distribution. In Figs. 1(c), 2(c), and 3(c) we collapse the data by rescaling  $x$  by its characteristic size  $x^*$ . All distributions are consistent with the scaling form of Eq. (1). The measured values of scaling exponents are summarized in Table I.

As shown in Fig. 2(b), the most probable traveling length  $\tilde{\ell}^*$  scales as  $\tilde{\ell}^* \sim r^{d_{\tilde{\ell}}}$  where  $d_{\tilde{\ell}}=1.21\pm 0.02$ . Note that  $d_{\tilde{\ell}}$  is significantly different from the minimal path exponent  $d_{min}=1.130\pm 0.002$  [15], while it is within the error bars of

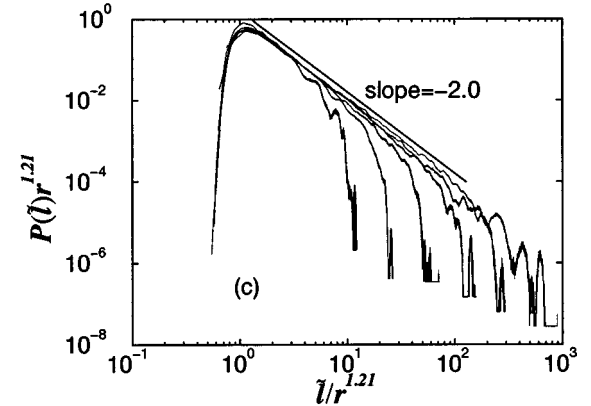
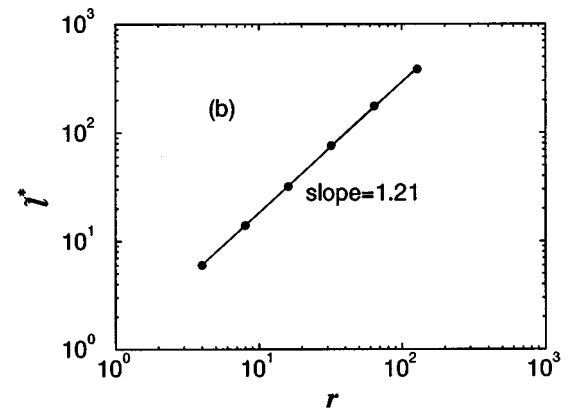
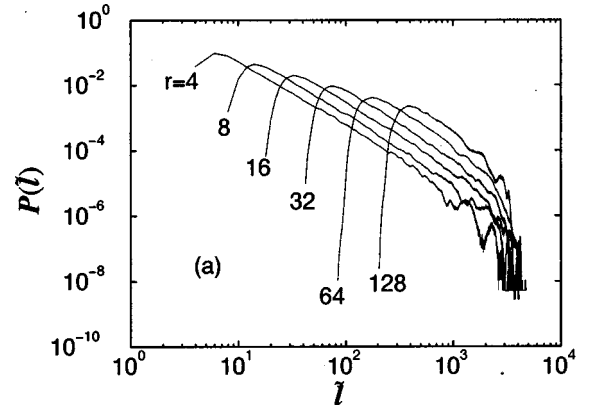


FIG. 2. (a) Log-log plot of traveling distance distribution  $P(\tilde{\ell})$  for  $r=4, 8, 16, 32, 64$ , and  $128$ . (b) Log-log plot of the most probable traveling length versus  $r$ . A linear fit yields  $d_{\tilde{\ell}}=1.21\pm 0.02$ . (c) The data obtained by rescaling the traveling length with its characteristic length  $\tilde{\ell}^* \sim r^{1.21}$ . A fit of the power-law regime gives  $g_{\tilde{\ell}}=2.0\pm 0.05$ .

the exponent for the optimal path in random energy landscapes,  $d_{opt}=1.2\pm 0.02$  [16], and the shortest path in invasion percolation with trapping,  $d_{opt}=1.22\pm 0.01$  [17].

In many transport problems, the characteristic time scales with the characteristic length with a power law,  $t^* \sim (\ell^*)^z$ . Since  $t^*$  scales as  $r^{d_t}$  and  $\ell^*$  scales as  $r^{d_{\ell}}$ , it is reasonable to assume that  $z=d_t/d_{\ell}$ . Combining this relation, the relation  $t_{min} \sim \ell_{min}^z$ , Eq. (1), and the identities  $P(\ell_{min})d\ell_{min}=P(t_{min})dt_{min}$  we obtain scaling relations between exponents,

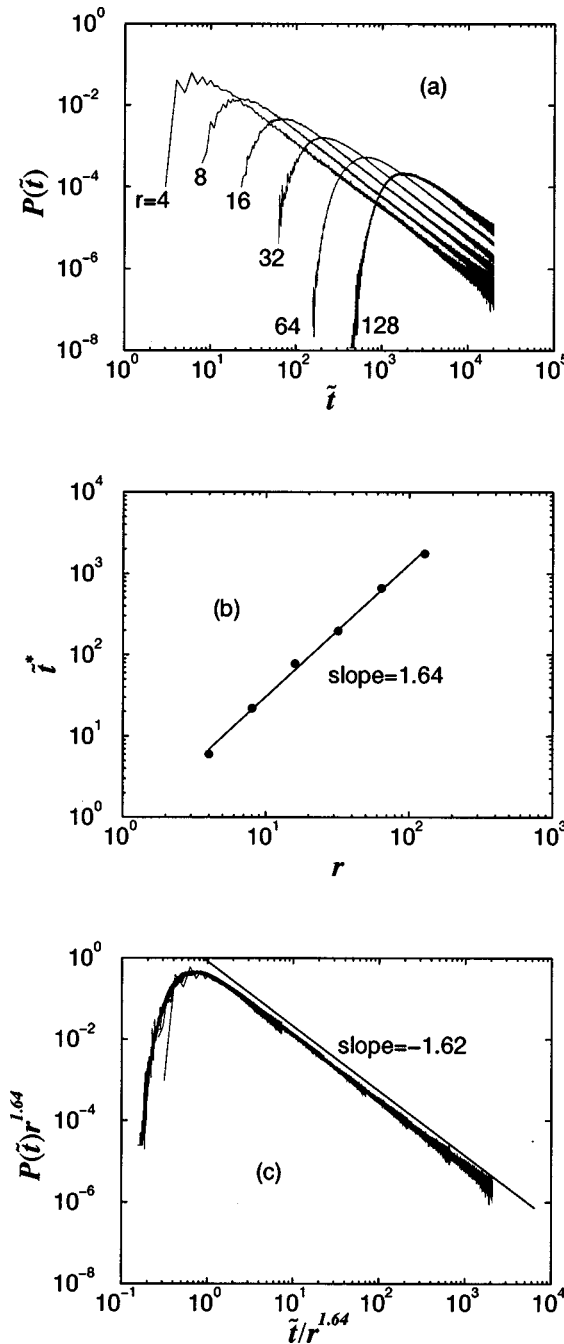


FIG. 3. (a) Log-log plot of traveling time distribution  $P(\tilde{t})$  for  $r=4, 8, 16, 32, 64$ , and  $128$ . (b) Log-log plot of the most probable time versus  $r$ . A linear fit yields  $d_{\tilde{t}}=1.64 \pm 0.02$ . (c) The data obtained by rescaling the time with its characteristic time  $\tilde{t}^* \sim r^{1.64}$ . A linear fit of the power-law regime gives  $g_{\tilde{t}}=1.62 \pm 0.05$ .

TABLE I. Results for the exponents. Our  $d=2$  results for  $d_{\ell_{min}}$  and  $g_{\ell_{min}}$  are within error bars of  $d_{min}$  and  $g'_x$  in Ref. [14]. For comparison, the theoretical values of  $d_x$  and  $g_x$  for  $d=6$  are all 2.

$x$	$d_x$	$g_x$
$\ell_{min}$	$1.13 \pm 0.01$	$2.14 \pm 0.05$
$t_{min}$	$1.33 \pm 0.05$	$1.90 \pm 0.05$
$\tilde{\ell}$	$1.21 \pm 0.02$	$2.00 \pm 0.05$
$\tilde{t}$	$1.64 \pm 0.02$	$1.62 \pm 0.05$

$$(g_{\ell_{min}} - 1)d_{\ell_{min}} = (g_{t_{min}} - 1)d_{t_{min}}, \quad (3)$$

This scaling relation is well satisfied by the set of scaling exponents given in Table I.

Because of flow conservation, the velocity at distance  $r'$  from point A should scale inversely proportional to the number of bonds at this distance, which scales as  $(r')^{d_B-1}$  where  $d_B$  is the fractal dimension of the transport backbone. Then, the traveling time for a particle to travel the distance  $r$  is given by

$$\tilde{t}^*(r) \sim \int_0^r \frac{1}{v(r')} dr' \sim r^{d_B}. \quad (4)$$

Note that  $\tilde{t}^*(r)$  is the most probable traveling time in our system, so we obtain the scaling relation  $d_{\tilde{t}}=d_B$ . Thus, the most probable traveling time is characterized by the transport backbone dimension of the media. This result is consistent with the homogeneous case, where  $d_B=2$ . The most recently reported value for the fractal dimension of the backbone is  $d_B=1.6432 \pm 0.0008$  [18] for  $d=2$ , which is in agreement with our results (Table I).

The minimal traveling time is the sum of inverse velocities over the fastest path where as noted above the fastest path is statistically identical to the shortest path. While the velocity distribution has been studied extensively [19] (e.g., it is known to be multifractal), because the velocities along the path are correlated, how the minimum traveling time distribution is related to the local velocity distribution is an open challenge for further research.

We thank A. Coniglio, D. Stauffer, and especially M. Barthélémy for fruitful discussions, and BP Amoco for financial support. We also thank J. Koplik and S. Redner for discussions concerning the limitation of a PLA.

[1] See, e.g., the comprehensive review by M. Sahimi, *Flow and Transport in Porous Media and Fractured Rock* (VCH, Boston, MA, 1995), and extensive references therein.  
[2] P. G. Saffman, *J. Fluid Mech.* **6**, 321 (1959).  
[3] J.-C. Bacri, J. P. Bouchaud, A. Georges, E. Guyon, J. P. Hulin, N. Rakotomalala, and D. Salin, in *Hydrodynamics of Dispersed Media*, edited by J. P. Hulin, A. M. Cazabat, E. Guyon,

and F. Carmona (Elsevier, Amsterdam, 1990), p. 249.  
[4] J. Koplik, S. Redner, and D. Wilkinson, *Phys. Rev. A* **37**, 2619 (1988).  
[5] *Fractals and Disordered Systems*, 2nd ed., edited by A. Bunde and S. Havlin (Springer, New York, 1996).  
[6] It is customary to model oil recovery for configurations in which the lateral extents are much greater than the vertical

extent using two-dimensional bond percolation.

[7] By passive tracer we mean that the tracer moves only by convection, ignoring molecular diffusion that is slow on the time scales of interest, and that it is not absorbed by its surroundings.

[8] Passive tracer dispersion with similar dipolar as well as multipolar geometries has been studied for homogeneous media by J. Koplik, S. Redner, and E. J. Hinch, *Phys. Rev. E* **50**, 4650 (1994).

[9] This normalization realistically models oil recovery where constant flow, as opposed to constant pressure, is maintained.

[10] A PLA is a useful approximation for any flow whose velocity field is known to be constant in time, but for which transport properties cannot be solved either analytically or numerically. A PLA is inaccurate for very large traveling times due to the low probability of entering bonds with low potential differences (and therefore long transit times; see also Ref. [4]). The “very long time regime” where diffusion becomes a significant factor is not considered in this paper.

[11] The traveling path is randomly selected with a probability out of all possible paths connecting two points. If the path contains  $n$  nodes, then the probability of the path is determined as a product of the independent local probabilities  $p_{ij}$  over the number of nodes.

[12] S. Havlin and D. Ben-Avraham, *Adv. Phys.* **36**, 695 (1987).

[13] P.-G. de Gennes, *Scaling Concepts in Polymer Physics* (Cornell University Press, Ithaca, NY, 1979).

[14] N. V. Dokholyan, S. V. Buldyrev, S. Havlin, P. R. King, Y. Lee, and H. E. Stanley, *J. Stat. Phys.* **93**, 603 (1998).

[15] H. J. Herrmann and H. E. Stanley, *J. Phys.* **21**, L829 (1988).

[16] M. Cieplak, A. Maritan, and J. R. Banavar, *Phys. Rev. Lett.* **72**, 2320 (1994); **76**, 3754 (1996).

[17] M. Porto, S. Havlin, S. Schwarzer, and A. Bunde, *Phys. Rev. Lett.* **79**, 4060 (1997).

[18] P. Grassberger, *Physica A* **262**, 251 (1999).

[19] L. de Arcangelis, S. Redner, and A. Coniglio, *Phys. Rev. B* **31**, 4725 (1985).